Probabilistic Cost-Benefit Analysis of Climate Change Adaptation Strategies for New RC Structures Exposed to Chloride Ingress

Emilio Bastidas-Arteaga, Mark G. Stewart

Probabilistic Cost-Benefit Analysis of Climate Change Adaptation Strategies for New RC Structures Exposed to Chloride Ingress

E. Bastidas-Arteaga
LUNAM Université, Université de Nantes-Ecole Centrale Nantes, GeM, Institute for Research in Civil and Mechanical Engineering/Sea and Littoral Research Institute, CNRS UMR 6183/FR 3473, Nantes, France

M.G. Stewart
The University of Newcastle, New South Wales, Australia

ABSTRACT: Reinforced concrete (RC) structures are subjected to environmental actions affecting their performance, serviceability and safety. Among these actions, chloride ingress leads to corrosion initiation and its interaction with service loading could reduce its operational life. Experimental evidence indicates that chloride ingress is highly influenced by weather conditions in the surrounding environment and therefore by climate change. Consequently, both structural design and maintenance should be adapted to these new environmental conditions. This work focuses on the assessment of the costs and benefits of a climate adaptation strategy for new RC structures placed in chloride-contaminated environments under various climate change scenarios. Their cost-effectiveness will be measured in terms of the Benefit-to-Cost Ratio (BCR) and the probability that BCR exceeds unity –i.e., Pr(BCR>1). BCR is selected because it seems to be a metric that government and policy makers are familiar with. The results indicate that the cost-effectiveness of a given adaptation strategy will depend mainly on exposure conditions and climate change scenarios.

1 INTRODUCTION

Concrete is the predominant construction material for buildings, bridges, wharves, and other infrastructure in Europe, Australia and elsewhere. A potentially important factor for asset management is the possible influence of climate change. This may alter the environment to which infrastructure is exposed, and in turn may alter the factors known to affect the corrosion of reinforcing steel, including temperature, humidity, ocean acidification, airborne pollutants, etc. Depending on the precise exposure conditions, each of these can influence initiation or progression of corrosion and thus have an effect on maintenance costs and remaining life. The annual cost of corrosion worldwide is estimated to exceed $1.8 trillion, which translates to 3% to 4% of the Gross Domestic Product (GDP) of industrialized countries (Schmitt 2009). Since the direct and indirect costs of corrosion are immense, a climate-change induced acceleration of the corrosion process by only a few percent can result in increased maintenance and repair costs of hundreds of billions of dollars annually.

Until recently all corrosion research assumed constant average climatic conditions for the development of deterioration models. This is still the case but some efforts have been made to consider the effect of changes in the parameters involved. For example, for atmospheric corrosion models CO_2 levels, time of wetness, temperature, humidity, etc. typically are modelled as stationary variables. However, even under an optimistic scenario where CO_2 emissions are abated to reduce temperature increases to 2˚C by 2100, IPCC (2007) reports that such a scenario (B1 or A1T) is likely only if non-fossil energy sources dominate. An increase in temperature will increase the rate of infiltration of deleterious substances (increased material diffusivity) and increase the corrosion rate of steel. A decrease in relative humidity may also increase the rate of infiltration of deleterious substances (Stewart et al. 2011). Typically these parameters must be considered as random variables or stochastic processes, and their statistical characteristics will gradually change with time. An appropriate framework for dealing with this problem is structural reliability and risk-based decision analysis.

A benefit of a probabilistic approach to damage prediction is that it enables a risk-based economic assessment of climate adaptation strategies. In addition to reducing environmental exposure as much as possible, practical adaptation solutions in new designs may come from increasing cover and strength grade, or any approaches that reduce material diffusion coefficient without compromising the reliability and serviceability of concrete. Stewart et al. (2012) considered the effect of climate adaptation strategies including increases in cover thickness, improved quality of concrete, and coatings and barriers on damage risks. It was found that an increase in design

cover of 10 mm and 5 mm for structures where carbonation or chlorides govern durability, respectively, will ameliorate the effects of a changing climate.

The present paper will extend this decision framework considerably to assess the costs and benefits of a climate adaptation measure to reduce the impact of chloride-induced corrosion damage: increase in design cover. The cost-effectiveness will be measured in terms of Benefit to Cost Ratio (BCR) equal to benefits divided by the cost. The stochastic analysis also enables the probability that BCR exceeds unity to be estimated as Pr(BCR>1). In this case, while mean BCR can be high, there may be a likelihood of BCR less than one (net loss) which is risk-averse decision-maker may need to consider when making a decision. The results of the paper will help provide practical advice to policy makers to help 'future proof' built infrastructure to a changing climate.

2 CLIMATE CHANGE MODELLING

The future climate is projected by defining carbon emission scenarios in relation to changes in population, economy, technology, energy, land use and agriculture, represented by a total of four scenario families, i.e., A1, A2, B1 and B2 (IPCC 2007). Subcategories of the A1 scenario included differing energy sources (fossil intensive, non-fossil energy and a balance across all sources, for example, A1FI, A1T and A1B, respectively). In addition, scenarios of CO_2 stabilisation at 450 and 550 ppm by 2150 were also introduced to consider the effect of policy intervention (Wigley et al. 1996). Hence, the A1FI, A1B and 550 ppm stabilisation scenarios represent high, medium emission scenarios and policy intervention scenarios, respectively.

The economic assessment of adaptation measures at any time *t* will be dependent on time-dependent changes in environmental parameters. The time-dependent trends in global median temperature increase are shown in Figure 1. Note that climate projections are relative to 1990 levels. It is observed from Figure 1 that the rate of temperature increase is low for all emission scenarios up to 2030, but the rate then increases dramatically for A1FI (high) emission scenario. On the other hand, the rate of temperature increase is lower for lower emission scenarios (A1B, 550 ppm by 2150), and the 550 ppm emission scenario begins to level out by 2100. Figure 1 also shows linear approximations where the linear approximations are quite reasonable for the lower emission scenarios (A1B, 550 ppm by 2150), but over-estimates predictions for the A1FI emission scenario. Since most climate projections are based on the 'likely' A1B emission scenario with increase in temperatures of 2-4˚C by 2100 (IPCC 2007), then a time-dependent increase in temperature is reasonable. A linear change in time-dependent RH is also assumed.

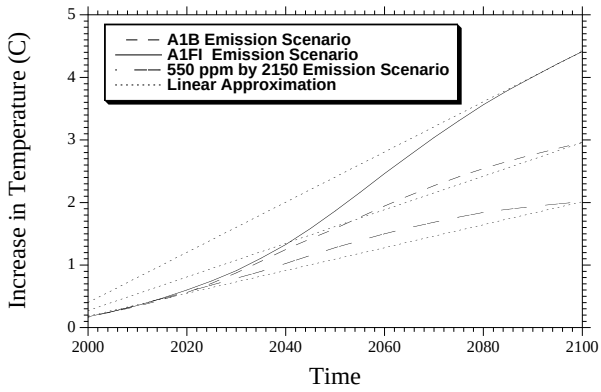

Figure 1. Increase in Median Global Temperature with Time, for Various Emission Scenarios.

Climate projections are subject to considerable uncertainty, and dependent on CO_2 emission scenarios and accuracy of global circulation models (GCM). IPCC (2007) projections of global temperature rises from the baseline of 1990 range from 1.1˚C (lower bound for 550 ppm by 2150 emission scenario) to 6.8˚C (upper bound for A1FI emission scenario). Projections for changes in relative humidity (RH) are less precise, however, the CSIRO Mk3.5 climate model predicts RH changes of -16.4% to +1.2% for Australia (Wang et al. 2012), and IPCC (2007) predicts reduced RH for Europe. For this reason, a scenario-based approach is used herein where results are presented for temperature changes of 0˚C to 6˚C in 100 years, and relative humidity changes of -20% to 10% 100 years. A scenario of no change in climate is also considered as engineering adaptation may make economic sense as a 'no regrets' policy even if climate predictions are wrong.

A comprehensive model of weather (humidity and temperature) should be integrated with deterioration models to assess the effects of a changing climate. Given the difficulties of integrating a fully coupled model of weather with a chloride ingress model, a simplified approach for modelling climate is considered in this study. It accounts for (i) influence of climate change, (ii) seasonal variations, and (iii) random nature of weather within a season. The formulation of this model is detailed in Bastidas-Arteaga et al. (2013).

3 DETERIORATION MODELLING

Deterioration modelling allows estimating the effects of chloride ingress with regard to serviceability or ultimate limit states. Ultimate limit states are highly dependent on both, geometrical characteristics (cross-sectional dimensions, span length, etc.) and loading (dead, live, seismic, etc.). Therefore, to generalise the results, this work focuses on a ser-

viceability limit state in which the cost-effectiveness of adaptation measures is evaluated in terms of its effect on the time to corrosion damage (severe cracking or spalling). Corrosion-induced cover cracking and damage occurs on the concrete surface above and parallel to the rebars. The time to corrosion damage, (severe cracking or spalling), T_{sp} is thus obtained as the sum of three stages: (i) corrosion initiation (T_i); (ii) crack initiation (T_{1st}, time to first cracking - hairline crack of 0.05 mm width), and; (iii) crack propagation (T_{sev}, time for crack to develop from crack initiation to a limit crack width, w_{lim}) – i.e., $T_{sp}=T_i+T_{1st}+T_{sev}$. After corrosion initiation, the kinematics of T_{1st} and T_{sev} is controlled by the corrosion propagation.

3.1 *Corrosion Initiation*

The time to corrosion initiation, T_i, is estimated by comparing the chloride concentration at the cover depth, c_t, with a threshold concentration for corrosion initiation C_{th}. The adopted chloride ingress model considers the interaction between three physical processes: *chloride ingress*, *moisture diffusion* and *heat transfer*. Each phenomenon is represented by a partial differential equation (PDE) expressed in the following general form (Bastidas-Arteaga et al. 2011):

$$\zeta \frac{\partial \psi}{\partial t} = \underbrace{\operatorname{div} J}_{\text{diffusion}} + \underbrace{\operatorname{div} J'}_{\text{convection}} \tag{1}$$

where ς represents the studied parameter, t is the time and the correspondence between ψ, J, J' and the terms for the physical problem is presented in Table 1.

Table 1. Correspondence between eq. (1) and the governing differential equations

Physical Process	ψ	ς	J	J'	q'^{s}_{ψ}
Chloride ingress	C_{fc}	1	$D_c^* \overrightarrow{\nabla} C_{fc}$	$C_{fc} D_h^* \overrightarrow{\nabla} h$	q_h^s
Moisture diffusion	h	$\partial w_e/\partial h$	$D_h^* \overrightarrow{\nabla} h$	0	0
Heat transfer	T	$\rho_c c_q$	$\lambda \overrightarrow{\nabla} T$	0	0

For chloride ingress, C_{fc} is the concentration of free chlorides, h is the relative humidity and D_c^* and D_h^* represent the apparent chloride and humidity diffusion coefficients, respectively:

$$D_c^* = D_{c,ref} \frac{f_1(T) f_2(t) f_3(h)}{1 + (1/w_e)(\partial C_{bc}/\partial C_{fc})} \tag{2}$$

$$D_h^* = D_{h,ref} \frac{g_1(h) g_2(T) g_3(t_e)}{1 + (1/w_e)(\partial C_{bc}/\partial C_{fc})} \tag{3}$$

where $D_{c,ref}$ and $D_{h,ref}$ are reference diffusion coefficients measured to standard conditions (Saetta et al. 1993), w_e is the evaporable water content, and f_i and g_i are correction functions to account for the effects of temperature, relative humidity, ageing and degree of hydration of concrete. These functions are detailed in Bastidas-Arteaga et al. (2011). The term $\partial C_{bc}/\partial C_{fc}$ represents the binding capacity of the cementitious system which relates the free and bound chlorides concentration at equilibrium. A Langmuir isotherm is used in this work. The constants of the isotherm are α_L=0.1185 and β_L=0.09.

For moisture diffusion, the humidity diffusion coefficient D_h is estimated by accounting for the influence of the parameters presented in eq. (3). The term $\partial w_e/\partial h$ (Table 1) represents the moisture capacity which relates the amount of free water, w_e, and the pore relative humidity, h. For a given temperature this relationship has been determined experimentally by adsorption isotherms. According to the Brunauer-Skalny-Bodor (BSB) model, the adsorption isotherm depends on temperature, water/cement ratio, w/c, and the degree of the hydration attained in the concrete, t_e. This work adopts the BSB model to represent the moisture capacity.

Finally, for heat transfer (Table 1) ρ_c is the concrete density, c_q is the concrete specific heat capacity, λ is the thermal conductivity of concrete, and T is the temperature inside the concrete after time t.

The flow of chlorides into concrete is estimated by solving simultaneously the system of equations described by eq. (1) and Table 1. The numerical approach used to solve the coupled system of PDEs combines a finite element formulation with finite difference to estimate the spatial and temporal variation of C_{fc}, h and T.

3.2 *Corrosion Propagation*

After corrosion initiation, the diameter reduction of reinforcing bars induced by corrosion can be estimated in terms of a change in the volumetric rate by using Faraday's law:

$$\begin{aligned} d_u(t) &= d_0 - 0.0232 \int_{t_{ini}}^{t} i_{corr}(t) dt \\ p(t) &= 0.0116 \alpha \int_{t_{ini}}^{t} i_{corr}(t) dt \end{aligned} \tag{4}$$

where $d_u(t)$ is the residual diameter of the reinforcing bar at time t for uniform corrosion in mm, d_0 is the initial diameter of the bar in mm, and $p(t)$ is the pit depth at time t in mm, α is the ratio between pitting and uniform corrosion depths, and $i_{corr}(t)$ is the time-variant corrosion rate (μA/cm^2). The remaining cross-sectional area of steel for pitting corrosion is computed herein considering the relationships proposed by (Val et al. 1997). Given the complexity of the corrosion process, i_{corr} depends on many factors such as concrete pH and availability of oxygen, and water in the corrosion cell. For instance, the optimum relative humidity for corrosion is 70-80%. This

study considers the following time-variant corrosion rate model that takes into account the effect of temperature changes (Duracrete 2000b; Duracrete 2000a):

$$i_{corr}(t) = i_{corr,20}[1 + K_c(T(t) - 20)] \quad (5)$$

where $i_{corr,20}$ is the corrosion rate at 20 ºC, $T(t)$ is the temperature at time t (in ºC) and K_c is a factor that depends on the value of $T(t)$. For instance, K_c=0.025 if $T(t)$<20ºC or K_c=0.073 if $T(t)$>20ºC. Corrosion rates are obtained from various sources (Duracrete 1998). The corrosion rate is assumed lognormally distributed with statistical parameters for a temperature of 20 ^{o}C given by Duracrete (1998).

3.3 *Crack Initiation and Propagation*

The time to crack initiation, T_{1st}, is based on the model by El Maaddawy & Soudki (2007). The time to severe cracking, T_{ser}, referred to herein is the time when concrete cover cracking reaches a limit crack width of 1 mm. Mullard & Stewart (2011) have modelled rate of crack propagation which includes a confinement factor (k_c) that represents an increase in crack propagation due to the lack of concrete confinement around external reinforcing bars. If the reinforcing bar is in an internal location then k_c=1, but for rebars located at edges and corners of RC structures then k_c is in the range of 1.2 to 1.4. For more details see Mullard & Stewart (2011).

The times of crack initiation and propagation depend on the corrosion rate. Therefore, eq. (5) is used herein to account for the time-dependency of these times on corrosion rate including climate change effects. They are also dependent on concrete strength – i.e., tensile concrete strength, f_t, and elastic modulus of concrete E_c. These parameters are computer in terms of the compressive strength, f_c. Concrete strength is time-variant, and the time-dependent increase in concrete compressive strength after one year using the ACI method is f_c=1.162f_c(28) where f_c(28) is the 28 day compressive strength (Stewart 1996). Time-dependent gains in strength beyond one year are not considered in the present analysis.

4 REPAIR STRATEGY AND DAMAGE RISKS

The cumulative distribution function for the time of first damage in the period [0, t] for original concrete is given as:

$$p_s(0,t) = \Pr\left[t \geq T_{sp}\right] \quad (6)$$

where T_{sp} is the time when concrete cover severely cracks (reaches limit crack width w_{lim}), and where the asset owner can specify the limit crack width as the criterion for repair.

A patch repair is the most common technique to repair corrosion damage in RC structures – e.g., (BRE 2003; Canisius et al. 2004). For a patch repair, the concrete cover is typically removed to approximately 25 mm past the steel bars (which are then cleaned of corrosion products) and a repair material is installed. The maintenance strategy assumes that (Stewart 2001):

- concrete is inspected at time intervals of Δt;
- patch repair is carried out immediately after corrosion damage has been discovered at time of i^{th} inspection at time iΔt;
- damage limit state exceedance results in entire RC surface being repaired;
- repair provides no improvement in durability performance of the repaired structure (i.e., it is repaired with the same cover and concrete quality as the original design specification);
- damage may re-occur during the remaining service life of the structure, i.e., multiple repairs may be needed. The maximum possible number of damage incidents is n_{max} = T/Δt.

In addition, the time-dependent damage risks of the repaired material will not be the same as the original material $p_s(t)$ due to changed temperature and humidity at the time of repair (i.e. when the concrete is new). Hence, the damage risk for repaired (new) concrete exposed to the environment for the first time at time of repair, t_{rep} = $i\Delta t$, will change depending on the new climatic conditions and time of repairs:

$$p_{si}(i\Delta t,t) = \Pr\left[t \geq T_{sp,i}\right] \quad (7)$$

where $T_{sp,i}$ is the time to severe cracking when new concrete is exposed to the environment for the first time after repair.

4.1 *Numerical example*

This example will illustrate the assessment of time-dependent damage risks for RC structures placed in a chloride-contaminated environment under various climate change scenarios. It is supposed that the studied RC structure will be exposed to chlorides in a splash and tidal zone. The climatic conditions are defined by an oceanic environment placed at a middle latitude (i.e., Europe) where the yearly mean temperature and relative humidity vary between the intervals [5ºC; 25ºC] and [0.6; 0.8], respectively. According to Eurocode 2 (European standard 2004), this condition corresponds to a XS3 exposure for which the design cover (including the allowable execution tolerance) is c_{t0}=55 mm if the structural lifecycle is 50 years. This example considers the minimum characteristic compressive strength of f'_{ck}=35 MPa recommended by the Eurocode 2.

The probabilistic models used to estimate both failure probability and PDF of the time to failure are

presented in Table 2. It is assumed that all the random variables are statistically independent.

Table 2. Probabilistic models of the random variables

Variable	Units	Distribution	Mean	COV
$D_{c,ref}$	m^2/s	log-normal	$3 \cdot 10^{-11}$	0.20
C_{env}	kg/m^3	log-normal	7.35	0.20
C_{th}	wt% cem.	normal[a]	0.5	0.20
cover	mm	normal[b]	55	0.25
$D_{h,ref}$	m^2/s	log-normal	$3 \cdot 10^{-10}$	0.20
λ	W/(m°C)	beta on [1.4;3.6]	2.5	0.20
c_q	J/(kg°C)	beta on [840;1170]	1000	0.10
ρ_c	kg/m^3	normal[a]	2400	0.04
$i_{corr-20}$	$\mu A/cm^2$	log-normal	2.586	0.67
α		gumbel	5.65	0.22
$f_c(28)$	MPa	normal[a]	$1.3(f'_{ck})$	0.18
f_t	MPa	normal[a]	$0.53(f_c)^{0.5}$	0.13
E_c	MPa	normal[a]	$4600(f_c)^{0.5}$	0.12

[a]truncated at 0, [b]truncated at 10mm

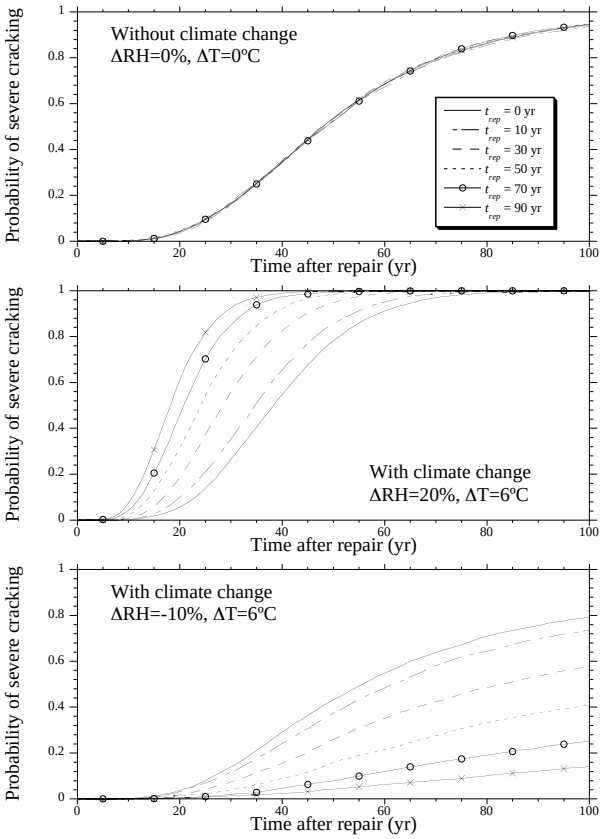

Figure 2. Probability of severe cracking for various climate change environments

Figure 2 clearly shows that the rate of damage risk is highly dependent on climate change effects. If climate change reduces the environmental relative humidity, i.e. ΔRH=-10% in 100 years, the chloride ingress mechanism slows down, and consequently, the probability of severe cracking decreases. An opposite behaviour is observed when climate change increases temperature and relative humidity.

For the modelled environmental conditions (splash and tidal zone in a middle latitude), damage risks are more sensitive to changes in relative humidity. Different sensitivities will be observed if the structure is subjected to other climate conditions. For instance, in tropical environments where there are no significant seasonal variations in temperature and relative humidity the effects of both on the probability of severe cracking will be different. Therefore, the time-dependency of damage risks should be considered for a comprehensive cost-benefit analysis of adaptation measures.

5 COST BENEFIT ANALYSIS

Costs and benefits may occur at different times so in order to obtain consistent results it is necessary for all costs and benefits to be discounted to a present value. If it is assumed that corrosion damage is always detected when the structure is inspected then the expected damage cost $E_{damage}(T)$ is the product of probability of corrosion damage and damage costs, i.e.,

$$E_{damage}(T) = \sum_{n=1}^{T/\Delta t} \sum_{i=n}^{T/\Delta} \left[p_{s,n}(i\Delta t) - p_{s,n}(i\Delta t - \Delta t) \right] \frac{C_{damage}}{(1+r)^{i\Delta t}} \quad (8)$$

where Δt is the time between inspections, n is the number of damage incidents, i is the number of inspection, $p_{s,n}(t)$ the probability of the n^{th} damage incidence before time t, C_{damage} is the cost of damage including maintenance and repair costs, user delay and disruption costs, and other direct or indirect losses arising from damage to infrastructure. For example, an asset owner should be able to quantify the unit repair cost ($\$/m^2$), and if the area of damage is known then repair cost can be estimated.

Equation (8) can be generalised for costs arising from multiple limit states, such as flexural failure, shear failure, etc. Corrosion damage (severe corrosion-induced cracking) is considered herein as the most influential mode of failure for the estimation of benefits. Equation (8) can be written in a different form as:

$$E_{damage}(T) = \sum_{i=1}^{T/\Delta t} \Delta P_{s,i} \frac{C_{damage}}{(1+r)^{i\Delta t}} \quad (9)$$

where $\Delta P_{s,i}$ is the probability of damage incident between the $(i-1)^{th}$ and i^{th} inspections which is a function of time since last repair which is turn is affected by damage risks for original and repaired concrete $p_s(0,t)$ and $p_{si}(i\Delta t,t)$, respectively. Eqn. (9) can be readily solved by Monte-Carlo simulation methods.

The risk reduction caused by an adaptation measure is thus:

$$\Delta R(T) = \frac{E_{damage-existing}(T) - E_{damage-adaptation}(T)}{E_{damage-existing}(T)} \quad (10)$$

where $E_{damage-existing}(T)$ and $E_{damage-adaptation}(T)$ are the cumulative expected damage cost (economic risk) for no adaptation measures (existing practice) and adaptation measures, respectively. If an adaptation measure is effective then $E_{damage-adaptation}(T)$ will be significantly lower than $E_{damage-existing}(T)$ resulting in

high risk reduction ΔR(T). In other words, ΔR(T) represents the proportional reduction in expected repair costs due to an adaptation measure.

Two criteria will be used to assess the cost-effectiveness of adaptation strategies: (i) Benefit-to-cost ratio or BCR and (ii) Probability of cost-effectiveness or Pr(BCR>1). The 'benefit' of an adaptation measure is the reduction in damages associated with the adaptation strategy, and the 'cost' is the cost of the adaptation strategy. The benefit-to-cost ratio BCR(T) is:

$$\mathrm{BCR}(\mathrm{T}) = \frac{\mathrm{E}_{\mathrm{damage-existing}}(\mathrm{T})\Delta\mathrm{R}(\mathrm{T})}{\mathrm{C}_{\mathrm{adapt}}} \quad (11)$$

where ΔR(T) is the reduction in risk caused by climate adaptation measures, C_{adapt} is the cost of adaptation measures that reduces risk by ΔR, and $E_{damage-existing}(T)$ is the cumulative expected damage cost (economic risk) for no adaptation measures (i.e, 'business as usual' or 'do nothing'). All costs are discounted to present values. Clearly, an adaptation measure that results in a benefit-to-cost ratio exceeding unity is a cost-effective adaptation measure. Since costs and benefits are time-dependent then it follows that benefit-to-cost ratio are time-dependent. Thus, an adaptation measure may not be cost-effective in the short-term, due to high cost for example, but the benefits may accrue over time resulting in cost-effectiveness in the longer-term.

The analysis assumes that many input variables are random variables (see Table 2) and so the output of the analysis (BCR) is also variable. This allows 10^{th} and 90^{th} percent lower and upper bounds of BCR to be calculated, as well as the probability that an adaptation measure is cost-effective at time T denoted herein as Pr(BCR>1).

For all adaptation options construction and repair cost data are needed, and such cost data is country, site and structure specific and so it is difficult to make generalisations about these costs. In this paper cost are expressed in 2012 U.S. dollars. It is assumed that design and inspection costs are similar for different adaptation measures and so are not needed for this comparative analysis. Hence, adaptation strategies will only affect the expected damage costs. As we are concerned about outdoor exposures then the external RC structural elements of interest are slabs, beams and columns. Corrosion damage is assumed to occur on one (exposed) face of a slab and beam, and all faces of a column.

5.1 *Cost of Damage (C_{damage})*

The cost of repair or replacement and associated user losses, etc. are considerable and for some structures user losses are often much greater than direct repair, replacement and maintenance costs. Val & Stewart (2003) assumed that the cost of RC bridge deck replacement is double the construction cost based on cost data for removal and replacement costs. However, this is likely to over-estimate the repair costs for most corrosion damage. The estimated cost for concrete patch repair using ordinary Portland cement is \$440/m^2 (Yunovivh et al. 2001; BRE 2003; Mullard & Stewart 2012). User losses and other user disruption costs are site and structure specific, but for many RC structures such costs will be minimised if the RC element to be repaired is an external structural member such as walls, columns or facade panels. However, for bridges closure of one lane for a four lane bridge can cause user delay costs of \$61,000 per day (Yunovivh et al. 2001). To allow for a minor user disruption cost the total failure cost is assumed as C_{damage}=\$500/m^2.

5.2 *Cost of Adaptation (C_{adapt})*

The baseline case for construction cost per unit volume (C_{cv}) including forms, concrete, reinforcement, finishing and labour is approximately \$750-\$1300/m^3, \$1400-\$1550/m^3 and \$1200-\$2400/m^3 for RC slabs (4.6-7.6 m span), RC beams (3.0-7.6 m span) and RC columns (300 mm × 300 mm to 900 mm × 900 mm), respectively (RSMeans 2012). It is assumed that an increase in design cover would increase cost of forms, concrete, reinforcement, finishing and labour by an amount proportional to the extra volume of concrete needed. Since C_{repair} units are \$/m^2 of surface area, but C_{cv} is given as per unit volume, then cost of construction (C_c) and C_{adapt} should be converted to cost per surface area exposed to deterioration, and so is corrected for structural member dimension such as element depth or column width (D). Table 3 describes the data and the relationships used to evaluate the adaptation costs. Identical formulations apply for RC square and circular columns where D is the column width or diameter, respectively.

Table 3. Data and relationships for the assessment of adaptation costs

	Slabs	Beams	Columns
D (mm)	100 to 300	200 to 800	300 to 900
C_{cv} (\$/m^3)	750-1,300	1,500	1,200-2,400
C_c	$C_{cv} \times D$ (m)	$C_{cv} \times D$ (m)	$C_{cv} \times D^2/4D$ (m)
C_{adapt}*	$C_c \times 1/D$ (mm)	$C_c \times 1/D$ (mm)	$C_c \times 4/D$ (mm)

*Per mm of extra cover

Table 4. Adaptation costs for various structural elements

Structural element	D (mm)	C_{adapt}* (\$/m^2)	5 mm increase (\$/m^2)	10 mm increase (\$/m^2)
Slabs	100	1.3	6.5	13
Slabs	300	0.75	3.75	7.50
Beams	200 to 800	1.5	7.5	15
Sq. columns	300	2.4	12	24
Sq. columns	600	1.55	7.7	15

*Per mm of extra cover

Based on the information given in Table 3, Table 4 presents the adaptation costs for various structural elements (per mm of extra cover). This table also presents the adaptation costs for 5 and 10 mm increase in extra cover. Clearly, adaptation costs are higher for a square column if cover is to be increased on all four faces of a square RC column, and damage can occur on all four faces.

5.3 *Illustrative example*

This section will illustrate the probabilistic assessment of the cost-effectiveness of adaptation strategies for a RC structure under the structural and exposure conditions described in Section 4.1. These results were computed for a discount rate r=4%. This value is within the range used by various government agencies – i.e. Australia 7%, U.S. 2-3%, UK Department of Transport, Sweden 4% and Finland 6% (Val & Stewart 2003).

Figure 3 presents the expected damage costs for existing cover and the two adaptation strategies for various climate change scenarios. The case without climate change, ΔRH=0% and ΔT=0ºC, is also presented in Figure 3. It is observed that the repair costs increase when both the variations in temperature and relative humidity are most important for the existing cover and the adaptation solutions. This is explained by the increase of chloride ingress rate when the structure is exposed to higher temperature and relative humidity (Bastidas-Arteaga et al. 2010). It is also noted that adaptation strategies reduce the mean repair costs because the number of repairs is reduced and/or the time to repair is longer when there is an increase of the concrete cover. It seems that a 10 mm increase of the design cover is the more effective adaptation strategy. However, these results cannot be used to compare the cost-effectiveness of an adaptation strategy because they do not include the adaptation costs. The adaptation costs will be considered in the following BCR study.

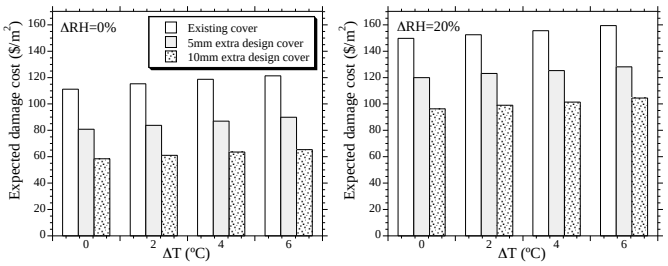

Figure 3. Expected damage costs for ΔRH=0% and ΔRH=20%

Figure 4 presents the cumulative probability of the BCR estimated for various structural components (slabs, beams and columns). The results correspond to a global warming scenario where ΔRH=20% and ΔT=6ºC in 100 years. The adaptation strategy presented herein consisted in increasing the design concrete cover by 5 mm. For all structural components, it is observed that the mean of the BCR is higher than 1 highlighting the benefits of considering this adaptation strategy. It is also noted that the Pr(BCR>1) is higher than 90%. This result indicates that the probability of having benefits if the adaptation measure is considered is very high for this kind of exposure and climate change scenario.

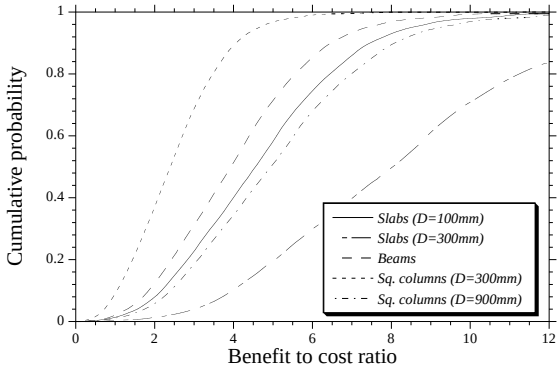

Figure 4. Pr(BCR) for several structural components and ΔRH=20% and ΔT=6ºC, for 5 mm increase cover

Tables 5 and 6 present the mean BCR and Pr(BCR>1) for various climate change scenarios and for a square column (300 × 300 mm) with all surfaces exposed to chlorides. These results indicate that the mean BCR is higher than one indicating that these adaptation measures provide benefits when compared to existing cover. When the uncertainties are included in the analysis, the results also show that Pr(BCR>1) are all higher than 63%. This indicates that the benefits of increasing concrete cover, for this aggressive environment, are important. Even if no climate change is expected, i.e. ΔRH=0% and ΔT=0˚C, the mean BCR>2 with a Pr(BCR>1)>80%.

On the other hand, as presented in Figure 2, some 'positive' effects of climate change on concrete durability could be attended if RH decreases with time. These positive effects will therefore reduce the costs-effectiveness of adaptation measures. For instance, if the relative humidity decreases (i.e., ΔRH=-10%), the chloride ingress rate will also decrease diminishing the number of repairs and consequently repair costs. In such a case, Table 5 indicates that the mean BCRs computed when ΔRH=-10% are generally lower than the computed for the case when ΔRH=0%. This means that the benefits of the adaptation measures could be lower under some climate change conditions. However, mean BCR still exceeds one. Therefore, the effects of climate adaptation measures should be carefully evaluated in order to decide if they provide benefits of losses with respect to the existing design.

Finally, comparing both adaptation strategies, it is noted that an increase of 5 mm cover provides higher estimates of BCR and Pr(BCR>1). Therefore, for this configuration under the above-defined environmental conditions an increase in design cover of 5 mm is recommended as a cost-effective climate change adaptation measure.

Table 5. BCR and Pr(BCR>1) (shown in italics), for $C_{a\text{-}dapt}$=\$12/m^2, and 5 mm Increase in design cover.

ΔRH	ΔT=0˚C	ΔT=2˚C	ΔT=4˚C	ΔT=6˚C
-10%	1.73 (*70%*)	2.26 (*90%*)	2.51 (*94%*)	2.62 (*94%*)
0%	2.53 (*89%*)	2.62 (*92%*)	2.64 (*94%*)	2.62 (*96%*)
10%	2.49 (*97%*)	2.41 (*97%*)	2.45 (*95%*)	2.46 (*96%*)
20%	2.49 (*95%*)	2.44 (*97%*)	2.52 (*96%*)	2.61 (*95%*)

Table 6. BCR and Pr(BCR>1) (shown in italics), for $C_{a\text{-}dapt}$=\$24/m^2, and 10 mm Increase in design cover.

ΔRH	ΔT=0˚C	ΔT=2˚C	ΔT=4˚C	ΔT=6˚C
-10%	1.54 (*63%*)	1.95 (*80%*)	2.17 (*86%*)	2.33 (*88%*)
0%	2.20 (*84%*)	2.26 (*89%*)	2.30 (*92%*)	2.33 (*94%*)
10%	2.20 (*94%*)	2.21 (*94%*)	2.19 (92%)	2.22 (*94%*)
20%	2.22 (*95%*)	2.23 (*95%*)	2.25 (*96%*)	2.29 (*94%*)

6 CONCLUSIONS

The kinematics of the chloride ingress and corrosion propagation mechanisms is highly influenced by the surrounding environmental conditions including climate change that could accelerate or decelerate these processes depending on specific exposure and environmental conditions. Therefore, damage risk assessment becomes time-dependent. These aspects should be considered on the assessment of the cost-effectiveness of adaptation strategies. For the illustrative example, it has been found that increasing of concrete cover by 5 or 10 mm is generally cost-effective with higher probabilities to obtain benefits. Under these conditions, a 5 mm increase of extra cover could provide a higher net benefit. Nevertheless, different conclusions could be drawn under other exposures and climate conditions.

ACKNOWLEDGEMENTS

The authors acknowledge the support of the University of Nantes and the LiRGeC (Institut Ligérien de Recherche en Génie Civil et Construction).

REFERENCES

Bastidas-Arteaga, E., Chateauneuf, A., Sánchez-Silva, M., Bressolette, P., & Schoefs, F. 2010. Influence of weather and global warming in chloride ingress into concrete: A stochastic approach. *Structural Safety* 32: p.238–249.

Bastidas-Arteaga, E., Chateauneuf, A., Sánchez-Silva, M., Bressolette, P., & Schoefs, F. 2011. A comprehensive probabilistic model of chloride ingress in unsaturated concrete. *Engineering Structures* 33: p.720–730.

Bastidas-Arteaga, E., Schoefs, F., Stewart, M.G., & Wang, X. 2013. Influence of global warming on durability of corroding RC structures: A probabilistic approach. *Engineering Structures* 51: p.259–266.

BRE. 2003. *Residual Life Models for Concrete Repair - Assessment of the Concrete Repair Process*. UK: Building Research Establishment.

Canisius, T.D.G., & Waleed, N. 2004. Concrete Patch Repairs Under Propped and Unpropped Implementation. *Structures and Buildings* 157(SB2): p.149–156.

Duracrete. 1998. *Modelling of Degradation, DuraCrete, EU - Brite EuRam III, Contract BRPR-CT95-0132, Project BE95-1347/R4-5*.

Duracrete. 2000a. *Probabilistic calculations. DuraCrete—probabilistic performance based durability design of concrete structures. EU—brite EuRam III. Contract BRPR-CT95-0132. Project BE95-1347/R12-13*.

Duracrete. 2000b. *Statistical quantification of the variables in the limit state functions, DuraCrete, EU - Brite EuRam III, Contract BRPR-CT95-0132, Project BE95-1347/R9*.

European standard. 2004. *Eurocode 1 and 2: Basis of design and actions on structures and design of concrete structures* AFNOR.

IPCC. 2007. *Climate Change 2007: The Physical Science Basis. Contribution of Working Group I to the Fourth Assessment Report of the Intergovernmental Panel on Climate Change* S. Solomon et al. (eds). Cambridge, United Kingdom and New York, NY, USA: Cambridge University Press.

El Maaddawy, T., & Soudki, K. 2007. A model for prediction of time from corrosion initiation to corrosion cracking. *Cement and Concrete Composites* 29(3): p.168–175.

Mullard, J.A., & Stewart, M.G. 2011. Corrosion-Induced Cover Cracking: New Test Data and Predictive Models. *ACI Structural Journal* 108(1): p.7179.

Mullard, J.A., & Stewart, M.G. 2012. Life-Cycle Cost Assessment of Maintenance Strategies for RC Structures in Chloride Environments. *Journal of Bridge Engineering ASCE* 17(2): p.353–362.

RSMeans. 2012. *RSMeans Building Construction Cost Data*. Kingston, MA: RSMeans.

Saetta, A., Scotta, R., & Vitaliani, R. 1993. Analysis of chloride diffusion into partially saturated concrete. *ACI Materials Journal* 90(5): p.441–451.

Schmitt, G. 2009. Global needs for knowledge dissemination, research, and development in materials deterioration and corrosion control.

Stewart, M.G, Wang, X., & Nguyen, M.N. 2012. Climate change adaptation for corrosion control of concrete infrastructure. *Structural Safety* 35(0): p.29–39.

Stewart, M.G, Wang, X., & Nguyen, M.N. 2011. Climate change impact and risks of concrete infrastructure deterioration. *Engineering Structures* 33(4): p.1326–1337.

Stewart, M.G. 1996. Optimisation of Serviceability Reliability for Structural Steel Beams. *Structural Safety* 18(2/3): p.225–238.

Stewart, M.G. 2001. Spalling Risks, Durability and Life-Cycle Costs for RC Buildings. In *International Conference on Safety, Risk and Reliability – Trends in Engineering*, 537–542. IABSE

Val, D.V., & Melchers, R.E. 1997. Reliability of deteriorating RC slab bridges. *Journal of Structural Engineering ASCE* 123(12): p.1638–1644.

Val, D.V., & Stewart, M.G. 2003. Life-cycle analysis of reinforced concrete structures in marine environments. *Structural safety* 25: p.343–362.

Wang, X., Stewart, M.G., & Nguyen, M. 2012. Impact of climate change on corrosion and damage to concrete infrastructure in Australia. *Climatic Change* 110(3-4): p.941–957.

Wigley, T.M.L., Richels, R., & Edmonds, J.A. 1996. Economic and environmental choices in the stabilization of atmospheric CO2 concentrations. *Nature* 379: p.240–243.

Yunovivh, M., Thompson, N.G., Balvanyos, T., Lave, L., & CC Technologies Laboratories Inc. 2001. *Corrosion Costs and Preventive Strategies in the United States*. Washington, D.C.